

# IRIS IDENTIFICATION BASED ON LOG-GABOR FILTERING

*Ramy Zewail<sup>1</sup>, Ahmed Seif<sup>d</sup>, Nadder Hamdy<sup>1</sup>, Magdy Saeb<sup>2</sup>*  
*Arab Academy for Science, Technology & Maritime Transport*  
*College of Engineering,*

1. Electronics & Communication Department

2. Computer Department

*Alexandria, EGYPT*

## **Abstract**

An accurate biometric identification system is a critical requirement in a variety of applications. Iris-based identification has been receiving a lot of attention since its introduction in 1992. However, some techniques have limitations in identifying persons accurately and efficiently.

In this work, a procedure that captures local and global characteristics of the iris, using a bank of Log-Gabor filters is proposed. We call the vector that stores these characteristics a feature descriptor or simply the iris descriptor. Our experimental results demonstrate that Log-Gabor filters identification capabilities outperform other procedures based on the basic Gabor filters.

**Keywords:** Biometrics, Iris, Identification, Log-Gabor, Verification, descriptor.

## **1. INTRODUCTION**

It has been over a century now, since Alphonse Beritillon first introduced the idea of using biometrics, human body measurements, for solving crimes [3]. Today, Biometric Recognition is one of the most promising and reliable ways to authenticate the identity of a person. A biometric system recognizes a person using specific physiological for example fingerprints, face, retina, and iris. Other methods include behavioral such as gait, and signature characteristics possessed by a person [4].

Among various human characteristics, the texture of the iris (that is the colored portion of the eye) has drawn attention over the past few decades [5]. The visual texture of human iris is determined by the chaotic morphogenetic processes during embryonic development. Iris is distinctive and unique for each person including identical twins and each eye [4].

There are a number of properties that enhance the suitability of the iris for use in automatic identification. One important feature is that the iris is inherently isolated and protected from the external environment. Moreover, being an internal organ of the eye, behind the cornea and the aqueous humor; it is almost impossible to surgically modify the iris without unacceptable risk of damage. Also, its physiological response to light provides a natural test against fake irises [1, 10].

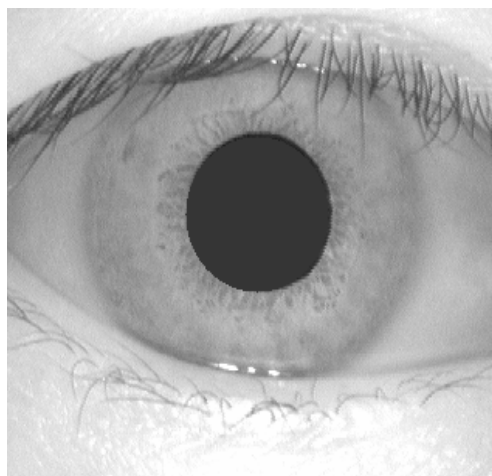


**Figure 1:** sample iris image from CASIA Database version 1.0

In the following sections, we present a modified procedure that is designed taking into consideration the high identification rate requirements of several civilian applications. Section 2 describes the required preprocessing steps. In section 3, we present the idea of using Log-Gabor filter bank for feature extraction. In section 4, experimental results are presented and compared with the use of “even symmetric” Gabor filters suggested in [2]. Finally, a summary and conclusion is shown in section 5.

## 2. THE PREPROCESSING STAGE

The iris representation for identification is required to be invariant to the changes in size of the pupil, different positions, and illumination conditions. The main steps in preprocessing stage are shown in block diagram in figure 2:

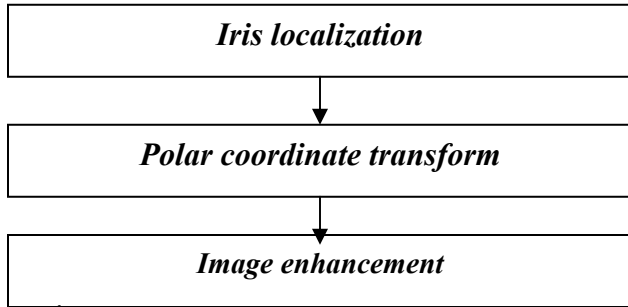


*Figure 2: Preprocessing stage block diagram*

### 2.1 Localizing the Iris

In this stage, the iris boundaries in the image of the eye are determined. It iris is the portion of the image between the pupil and the sclera and outside the pupil [6]. The process includes two steps: intensity adjustment and edge detection.

Intensity adjustment maps an image's intensity values to a new range. We apply power law transformation, equation 2.1,

$$s = cr^\gamma \quad 2.1$$

Where  $s$ ,  $r$  is the gray level of the output image, and the input image respectively,  $c$  and  $\gamma$  are positive constants. Afterwards, we apply “Canny edge detection” technique, The Canny method finds edges by looking for local maxima of the gradient of the image. The gradient is calculated using the derivative of a Gaussian filter. Two thresholds are used to detect strong and weak edges. Weak edges are only included in the output if they are connected to strong edges. This method is therefore less likely than others to be fooled by noise, and more is likely to detect true weak edges [11]. Finally, extraction is performed taking in consideration the circular nature of the iris image as shown in figure 3.

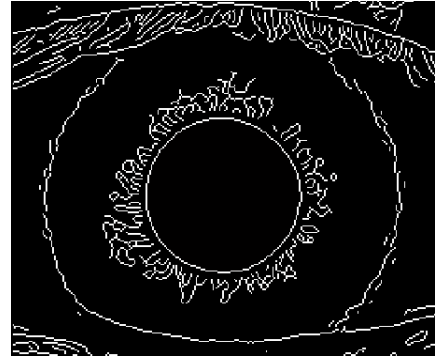


*Figure 3: Iris image after edge detection*

### 2.2 Cartesian to Polar Transformation

The localized Iris part is then transformed into polar coordinates, as shown in figure 4, to compensate for variations due to change of camera to eye distance. Moreover, the polar coordinate system compensates automatically for the stretching of iris tissue as the pupil dilates [7]. The image is then divided into 16 equal sub images. Lastly, the front part is eliminated to minimize the effect of eyelids overlap.



*Figure 4: Iris image in the polar coordinates*

### 2.3 Image enhancement

Image enhancement is necessary in order to compensate for the effects of some factors like image contrast, illumination and sensor noise.

We apply histogram equalization to enhance the histogram of the input image which is narrow and centered in the middle of the gray scale. This step enhances the image contrast. Subsequently, we apply a rotationally symmetric Gaussian low pass filter whose cutoff frequency depends on the energy distribution in the frequency domain. The filter equation is shown below.

$$h(x, y) = \frac{h_g(x, y)}{\sum_y \sum_x h_g} \quad 2.2$$

Where  $h_g$  is defined as:

$$h_g(x, y) = \exp\left\{-\frac{(x^2 + y^2)}{2\sigma^2}\right\} \quad 2.3$$

### 3. FEATURE EXTRACTION

On summarizes the major stages of the feature extraction procedure as shown in figure 5:

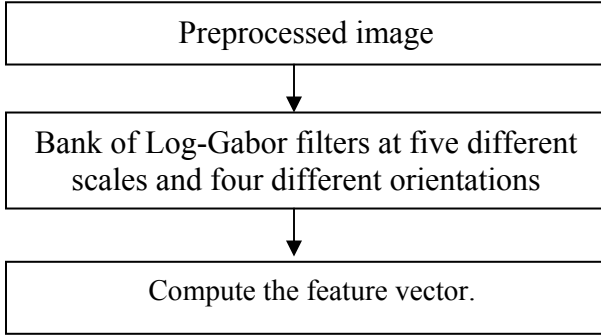


*Figure 5: Feature extraction block diagram*

#### 3.1 Log Gabor Filters

Gabor filters have been used extensively in a variety of image processing problems, such as fingerprint enhancement [4] and iris recognition [1, 2]. The Gabor function's most interesting property is that it achieves the lower bound in the Gabor-Heisenberg-Weyl uncertainty relation between space and spatial frequency. Thus the optimum compromise, in the problem of obtaining simultaneous localization in space and frequency, is obtained with the Gabor filter. Consequently, Gabor filters have been used intensively for texture analysis [4, 8].

The log Gabor function, as described in [9], is a modification to the basic Gabor function, in that the frequency response is a Gaussian on a log frequency axis, as defined:

$$G(f) = \exp\left\{-\frac{[\log(f/f_0)]^2}{2[\log(\sigma/f_0)]^2}\right\} \quad 3.1$$

The log Gabor function has the advantage of the symmetry on the log frequency axis. The log axis, as pointed out in [9], is the optimum method for representing spatial frequency response of visual cortical neurons. The Log-Gabor filters spread

information equally across the channels as shown in figure 6-b [9]. On the contrary, ordinary-Gabor filters over-represent low frequencies. As a result, it introduces redundancy in the response of low frequencies [9] as shown in figure 6-a.

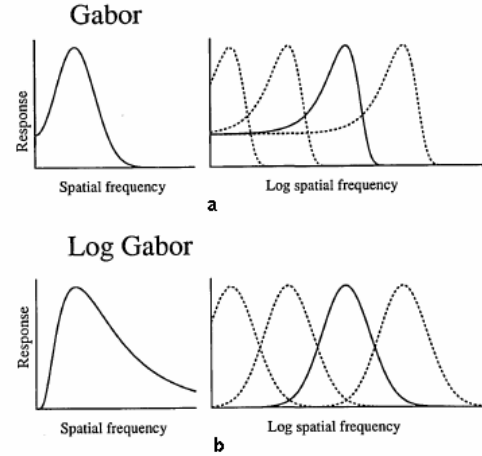


*Figure 6: Comparison of the Gabor and log Gabor function [9]*

#### 3.2 Image filtering

As mentioned before, the processed image is filtered in a bank of log Gabor filters at five different scales and four orientations. The filters parameters are chosen to get even coverage of the spectrum. Figure 7 illustrates the log Gabor filters for the same scale and different orientations.



*Figure 7: Log Gabor filters at different orientations*

The response of the filters at different orientations is shown in figure 8.



*Figure 8: Response of the filters at different orientations*

### 3.3 Generation of feature vector or descriptor

The average absolute deviation of gray values in the response of each filter is then calculated using equation 3.2.

$$D = \frac{1}{N} \left( \sum |f(x, y) - \mu| \right) \quad 3.2$$

The symbol N represents the number of pixels in the response,  $\mu$  is the mean of the response, and  $f(x, y)$  is the value of response at point x and y. Finally, a feature vector of length 320 entries is generated for each iris in our database. A sample of the iris feature vector is shown in figure 9.

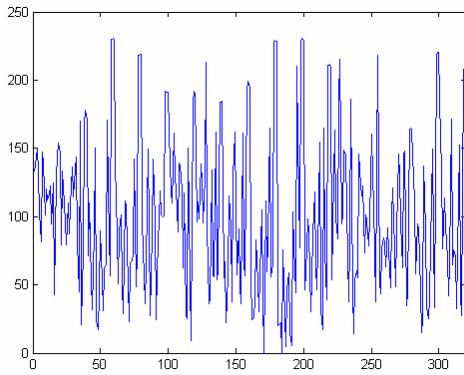


**Figure 9:** A sample of the 320-entry-long Feature vector or descriptor.

### 4. EXPERIMENTAL RESULTS

The experiments employ a database of 245 images collected from 35 persons, and 7 samples from each in two different sessions. This database was obtained from national laboratory of pattern recognition, Chinese Academy of Science. The algorithm has been tested in both identification (1: N) and verification (1: 1) modes.

To test the proposed algorithm in the verification mode, the samples were divided into two groups for training and testing. The training group is used to generate a template codebook. Next, each sample image of the testing set was then compared with all images in the template codebook. The matching was done using Euclidean distance. The distribution of the genuine or authorized matches and that of the

imposter matches were then estimated, and shown in figure 10.

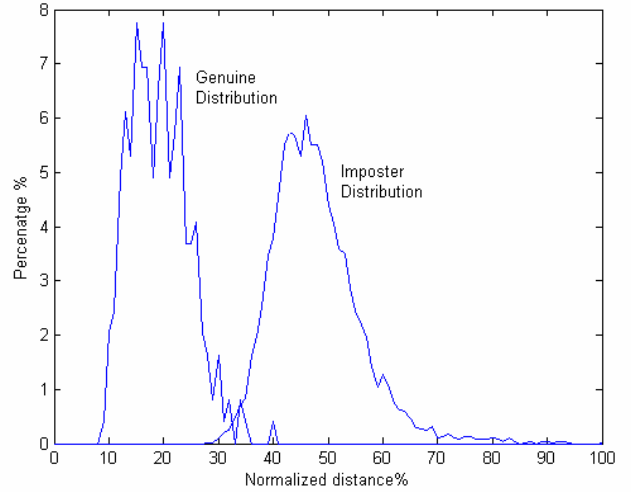


**Figure 10:** Genuine and Imposter Distribution

For a given distance threshold, the genuine accept rate and false accept rate can be calculated. A Receiver Operating Characteristic (ROC) was generated, that is a plot of Genuine Acceptance Rate (GAR) against False Acceptance Rate (FAR) for all possible distance thresholds. Figure 11 shows this ROC curve.

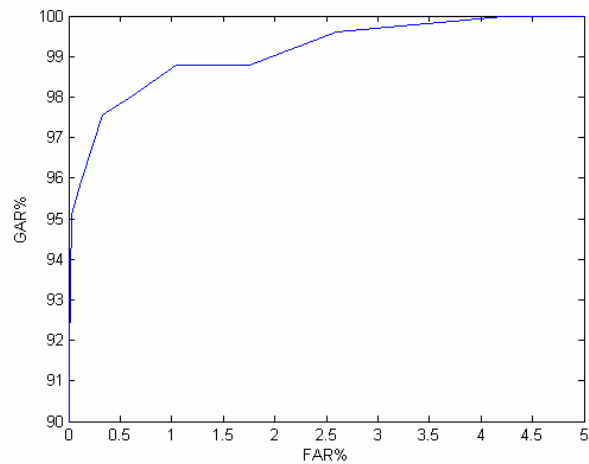


**Figure 11:** ROC curve (GAR vs FAR)

For the Identification mode, a nearest-neighbor classifier, decision based on the minimum Euclidean distance, was employed for matching with samples

divided into training and testing groups. The number of training samples was made variable and an identification rate was calculated each time. The performance of our algorithm has been compared with the even-symmetric Gabor filtering algorithm proposed in [2]. The detailed results are shown in table below.

**Table 1. :** Comparing Experimental Results for Identification mode

<b>Number of training samples</b>	<b>Identification rate: Log Gabor filtering</b>	<b>Identification rate: Even symmetric Gabor filtering</b>
4	99.6 %	98.7 %
3	97.6 %	95.9 %
2	96.7 %	94.3 %
1	89.0 %	82.1 %

#### 4. SUMMARY AND CONCLUSIONS

In this work we have developed a modified procedure for iris feature extraction based on Log-Gabor filter. The method, as shown before, can be summarized as follows:

- a. The preprocessing phase that embraces the following: localizing the iris, converting the co-ordinate system into polar form, and enhancement of the image.
- b. The feature extraction stage that includes: filtering the preprocessed image in four different orientations and five different scales using a bank of Log-Gabor filters, subsequently computing the average absolute deviation of the gray-scale values of the filter bank responses.

Based on the results of our experimentations, shown in section 4, one concludes that the procedure proposed reliable and accurate system for iris

identification based on log Gabor filtering. This filter produces an uncorrelated and less redundant representation for iris texture compared with the ordinary Gabor filters. The method achieved correct tracking of local and global features of iris images. Moreover, it produces very high identification results that are suitable for methodical search in large databases and access control. Future directions of our work include tracking more local information based on the information content distribution of the iris images.

#### Acknowledgment

The authors wish to acknowledge the kind cooperation of the Institute of Automation, Chinese Academy of Sciences for providing the CASIA Iris Database version 1.0 utilized in this work.

#### REFERENCES

- [1] Daugman J., "High confidence personal identification by rapid video analysis of iris texture," Proc. of the IEEE, International Carnahan conf. on security technology, 1992.
- [2] Ma L., Wang Y., Tan T., "Iris Recognition Based on Multi-channel Gabor Filtering," Proceedings of ACCV'2002, vol. I, pp.279-283, 2002.
- [3] Rhodes H., Bertillon A. : Father of Scientific Detection, Abelard-Schuman, New York, 1956.
- [4] Matnoni D., Maio D., Jain A.K., Prabhakar S., Handbook of fingerprint recognition, Springer-verlag, 2003
- [5] Daugman J, Recognizing Persons by Their Iris Patterns, Chapter 5 in Jain A., Bolle R., Pankanti S., Biometrics: Personal Identification in Networked Society, Kluwer Academic Publishers, 1999.
- [6] Shinyoung L., Kwanyong L., Okhwan B., and Taiyun K., "Efficient Iris Recognition through Improvement of Feature Vector and Classifier," *ETRI J.*, Vol.23, No.2, 2001.
- [7] Daugman J, "Demodulation by Complex-Valued Wavelets for Stochastic Pattern Recognition", International Journal of Wavelets, Multi-resolution and Information Processing Vol. 1, No. 1, 2003.
- [8] Gabor D., "Theory of communication," Journal IEE, Vol.93, n° III, 1946.
- [9] Field D., "Relations between the Statistics of Natural Images and the Response Properties of Cortical Cells," Journal of the Optical Society of America A, Vol. 4, No. 12, pp 2379-2394, December 1987.
- [10] Wildes R., "Iris Recognition: An Emerging Biometric Technology," *Proceedings of the IEEE*, vol.85, pp.1348-1363, Sept. 1997.
- [11] Canny J. "A Computational Approach to Edge Detection," IEEE Transactions on Pattern Analysis and Machine Intelligence, 1986. Vol. PAMI-8, No. 6, pp. 679-698.